

## High-performance MOCVD-SiN<sub>x</sub>/AlN/GaN MIS-HEMTs with low noise and high linearity for millimeter waves

YUAN Jing<sup>1,2</sup>, JING Guan-Jun<sup>1,2</sup>, WANG Jian-Chao<sup>1,2</sup>, WANG Liu<sup>1,2</sup>, GAO Run-Hua<sup>1</sup>,  
ZHANG Yi-Chuan<sup>1</sup>, YAO Yi-Xu<sup>1,2</sup>, WEI Ke<sup>1</sup>, LI Yan-Kui<sup>1</sup>, CHEN Xiao-Juan<sup>1\*</sup>

- (1. High-Frequency High-Voltage Device and Integrated Circuits R&D Center, Institute of Microelectronics of Chinese Academy of Sciences, Beijing 100029, China;  
2. University of Chinese Academy of Sciences, Beijing 100029, China)

**Abstract:** In this paper, we demonstrated SiN<sub>x</sub>/AlN/GaN metal-insulator-semiconductor high electron mobility transistors (MIS-HEMTs) with low noise and high linearity, by in-situ growth of SiN<sub>x</sub> gate dielectrics on ultra-thin barrier AlN/GaN heterostructure. Deep-level transient spectroscopy (DLTS) shows a traps-level depth of 0.236 eV, a capture cross-section of  $3.06 \times 10^{-19} \text{ cm}^2$ , and an extracted interface state density of  $10^{10} \sim 10^{12} \text{ cm}^{-2} \text{ eV}^{-1}$ , which confirms that the grown SiN<sub>x</sub> can reduce the interface state. The devices exhibit excellent DC, small signal, and power performance, with a maximum saturation output current ( $I_{\text{dmax}}$ ) of 2.2 A/mm at the gate voltage ( $V_{\text{gs}}$ ) of 2 V and the gate length of 0.15  $\mu\text{m}$ , a maximum current cutoff frequency ( $f_{\text{t}}$ ) of 65 GHz, a maximum power cutoff frequency ( $f_{\text{MAX}}$ ) of 123 GHz, a minimum noise figure ( $NF_{\text{min}}$ ) of the device of 1.07 dB and the gain of 9.93 dB at 40 GHz. The two-tone measurements at the  $V_{\text{ds}}$  of 6 V, yield a third-order intermodulation output power ( $OIP3$ ) of 32.6 dBm, and  $OIP3/P_{\text{dc}}$  of 11.2 dB. Benefited from the high-quality SiN<sub>x</sub>/AlN interface, the MIS-HEMTs exhibited excellent low noise and high linearity, revealing its potential in applications of millimeter waves.

**Key words:** SiN<sub>x</sub> gate dielectrics, MOCVD, MIS-HEMTs, interface state, low noise, linearity, millimeter waves

## 具有低噪声及高线性度的高性能 MOCVD-SiN<sub>x</sub>/AlN/GaN 毫米波 MIS-HEMTs

袁 静<sup>1,2</sup>, 景冠军<sup>1,2</sup>, 王建超<sup>1,2</sup>, 汪 柳<sup>1,2</sup>, 高润华<sup>1</sup>, 张一川<sup>1</sup>, 姚毅旭<sup>1,2</sup>, 魏 珂<sup>1</sup>,  
李艳奎<sup>1</sup>, 陈晓娟<sup>1\*</sup>

- (1. 中国科学院微电子研究所 高频高压器件与集成研发中心, 北京 100029;  
2. 中国科学院大学, 北京 100029)

**摘要:** 文章在超薄势垒 AlN/GaN 异质结构上采用金属有机化学气相沉积(MOCVD)原位生长 SiN<sub>x</sub> 栅介质, 成功制备了高性能的 SiN<sub>x</sub>/AlN/GaN 金属-绝缘体-半导体高电子迁移率晶体管(MIS-HEMTs)。深能级瞬态谱(DLTS)技术测试 SiN<sub>x</sub>/AlN 的界面信息, 显示其缺陷能级深度为 0.236 eV, 俘获截面为  $3.06 \times 10^{-19} \text{ cm}^2$ , 提取的界面态密度为  $10^{10} \sim 10^{12} \text{ cm}^{-2} \text{ eV}^{-1}$ , 表明 MOCVD 原位生长的 SiN<sub>x</sub> 可以有效降低界面态。同时器件表现出优越的直流、小信号和噪声性能。栅长为 0.15  $\mu\text{m}$  的器件在 2 V 的栅极电压 ( $V_{\text{gs}}$ ) 下具有 2.2 A/mm 的最大饱和输出电流, 峰值跨导为 506 mS/mm, 最大电流截止频率 ( $f_{\text{t}}$ ) 和最大功率截止频率 ( $f_{\text{MAX}}$ ) 分别达到了 65 GHz 和 123 GHz, 40 GHz 下的最小噪声系数 ( $NF_{\text{min}}$ ) 为 1.07 dB, 增益为 9.93 dB。  $V_{\text{ds}} = 6 \text{ V}$  时对器件进行双音测试, 器件的三阶交

Received date: 2023- 07- 14, revised date: 2023- 10- 10

收稿日期: 2023- 07- 14, 修回日期: 2023- 10- 10

**Foundation items:** Supported by the National Natural Science Foundation of China (62304252); the Youth Innovation Promotion Association of Chinese Academy Sciences (CAS) and IMECAS-HKUST-Joint Laboratory of Microelectronics

**Biography:** YUAN Jing (1999-), female, Hebei China, master. Research area involves GaN millimeter-wave low-noise devices and MMIC. E-mail: yuan-jing@ime.ac.cn

\* **Corresponding author:** E-mail: chenxiaojuan@ime.ac.cn

调输出功率 ( $OIP3$ ) 为 32.6 dBm,  $OIP3/P_{dc}$  达到 11.2 dB。得益于高质量的 SiN<sub>x</sub>/AlN 界面, SiN<sub>x</sub>/AlN/GaN MIS-HEMT 显示出了卓越的低噪声及高线性度, 在毫米波领域具有一定的应用潜力。

**关键词:** SiN<sub>x</sub> 栅介质; MOCVD; MIS-HEMTs; 界面态; 低噪声; 线性度; 毫米波

**中图分类号:** O48      **文献标识码:** A

## Introduction

Gallium nitride (GaN) based devices have been widely researched due to their advantages of high electron mobility, high breakdown voltage and high thermal conductivity, which can simplify the system of low-noise amplifiers and satisfy the requirements of circuit integration.

With the development of communication technology, the need of higher frequency for large bandwidth and lower noise is increasing<sup>[1]</sup>. The size of the device is continuously scaling down as its working frequency rises, and the short channel effect that eventually appears weakens the capacity of the gate to control the channel. Traditional AlGaIn/GaN HEMTs often reduce the aspect ratio by etching the gate slot to suppress the short channel effect. However, the etching process results in damages on the surface of AlGaIn, which leads to the current collapse effect of the device and worsen the noise performance of the device. Therefore, the research of AlN thin barrier devices with stronger polarization effects in the field of noise has a certain value. Compared with AlGaIn/GaN HEMTs, AlN/GaN HEMTs have stronger polarization and wider conduction band gap for lower probability of electrons entering the barrier layer in the channel. On this basis, gate dielectrics can effectively improve the interface quality of the device and further improve the noise performance. The selection of gate dielectrics and growth methods are crucial for device performance. In 2014, X. Lu<sup>[2]</sup> of the Hong Kong University of Science and Technology used MOCVD technology to grow SiN<sub>x</sub> gate dielectric layer in situ on AlN/GaN heterojunction, the measurement showed that the SiN<sub>x</sub>/AlN interface state presented  $10^{11} - 10^{12} \text{ cm}^{-2} \text{ eV}^{-1}$  low trap state densities. Therefore, MOCVD in situ growth of gate dielectric has certain significance for the research and development of low-noise devices.

At present, the research of GaN low-noise devices not only focuses on the improvement of the material growth and manufacturing processes, but also on the optimization of the device materials and structures, such as the choice of barrier layer materials, the optimization of heterostructure structure, etc. France F. Medjdoub *et al.*<sup>[1]</sup> adopted the AlN/GaN/AlGaIn double-heterostructure structure on Si-based GaN, with a gate length of 80 nm, and achieved a gain of 7.5 dB and a minimum noise figure of less than 1 dB at 36 GHz in 2012. The article published in NANO LETTERS in 2020 by Choi Woojin *et al.*<sup>[3]</sup> reported the purpose of Fin field effect transistor (Fin-FET) applied to millimeter wave low noise amplifiers to obtain greater transconductance and reduce knee point voltage by shortening the source/drain spacing. The measurement showed that the device had a minimum

noise figure of 2.2 dB at 30 GHz, and the linearity of the low-noise device was measured at 30 GHz with  $OIP3/P_{dc} \geq 8.2 \text{ dB}$ .

In this paper, based on the GaN process, AlN/GaN heterostructure was grown epitaxially on SiC substrate, and SiN<sub>x</sub> was grown in situ as gate dielectrics by MOCVD, high-quality gate dielectric material was obtained, and good interface characteristics were achieved. In addition, the AlN/GaN MIS-HEMTs with good noise performance applied in the millimeter wave frequency band were obtained by combining ohmic contact and the T-gate fabrication process. Deep-level transient spectroscopy (DLTS) technology was used to character the information of the device's gate dielectric material. Besides, the electrical properties such as DC output, small signal, noise, gain and linearity were evaluated.

## 1 Experiments

### 1.1 AlN/GaN heterostructure design

The short channel effect of the conventional AlGaIn/GaN HEMT device is more apparent as the operating frequency of the device rises, and the gate length gradually shortens. In contrast, the thin barrier AlN material can achieve a higher density in two-dimensional electron gas with the AlN thickness of only 3-5 nanometers due to a stronger polarization effect.

The energy bands of SiN<sub>x</sub>/AlN/GaN heterostructure with different AlN thicknesses were simulated. The simulation result of the heterostructure is shown in Fig. 1(a), Fig. 1(b) demonstrates the relationship between the 2DEG density and the AlN barrier thickness. It is challenging to create the two-dimensional electron gas when the AlN thickness is 3 nm because no clear potential well forms. However, the potential well becomes increasingly apparent as the barrier thickness rises. As the thickness of the barrier layer increases, the 2DEG surface density rapidly increases and gradually approaches saturation. When the thickness of the AlN barrier is selected as 5 nm, the simulation results show that the 2DEG surface density is  $1.98 \times 10^{13} \text{ cm}^{-2}$ .

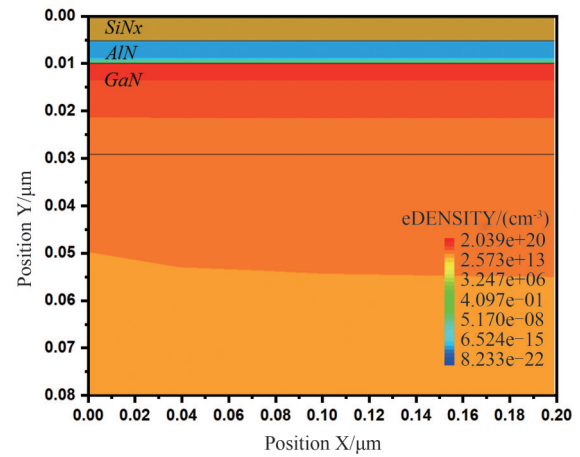
Thin barrier AlN/GaN heterostructure can be employed to satisfy millimeter wave application requirements without the necessity for etching, preventing the noise degradation and damage brought on by the etching process. Nevertheless, due to the lattice mismatch between the AlN and GaN materials up to 2.4%, the excessive thickness of AlN leads to the excessive stress of the material, and the strain relaxation is easy to crack during the growth of the material, which seriously affects the quality of the material. The barrier layer was chosen to be 5 nm, taking into account the actual application and

the concentration of the two-dimensional electron gas, and the  $\text{SiN}_x$  cap layer was generated in-situ to shield the AlN barrier layer from oxidation, contaminants, and water vapor adsorption.

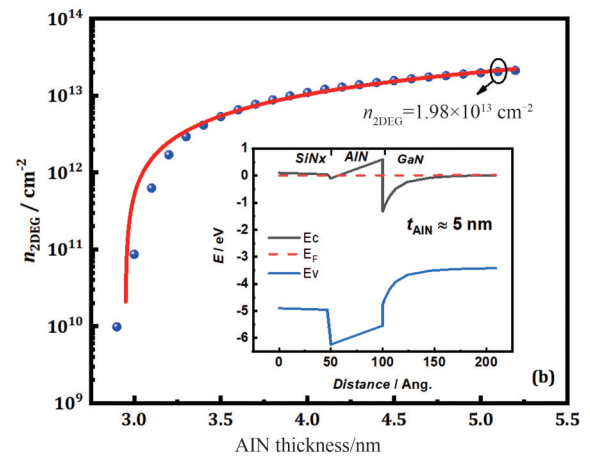
### 1.2 Main structure of device

The low-noise device is shown in Fig. 2(a), this paper used MOCVD in-situ growth technology to grow  $\text{SiN}_x$  gate dielectrics, high quality dielectric material was obtained, and robust  $\text{SiN}_x/\text{AlN}$  interface was achieved. The main function of the gate dielectric material is as follows: Firstly, due to the good insulation and high-quality  $\text{SiN}_x/\text{AlN}$  interface characteristics of in-situ grown  $\text{SiN}_x$ , it reduces the probability of electrons tunneling the barrier layer and injecting into the channel, reducing the collision of carriers in the channel, thus reducing the alloy scattering, and improving the mobility; Secondly, in-situ grown  $\text{SiN}_x$  improves the interface quality of the AlN barrier layer to suppress the interface state, thus reducing gate leakage and noise. SiC with a high lattice matching degree and high thermal conductivity was selected as the substrate layer of the device. In order to further reduce the interface tension and thermal mismatch caused by lattice mismatch, the AlN nucleating layer is grown, which can reduce the current collapse caused by interface mismatch, defect or trap effect, and reduce the noise of the device. Finally, the passivation layer of  $\text{SiN}_x$  can reduce the leakage current of the gate and increase the concentration of two-dimensional electron gas. In order to satisfy the millimeter-wave operation requirements of the device, the 150 nm T-shaped gate is adopted. As shown in Fig. 2(b) below, the gate resistance is reduced by increasing the gate cap structure to reduce the noise.

In this paper, after  $\text{SiN}_x$  was grown in situ on AlN/GaN heterojunction using MOCVD technology, the source and drain metal Ti/Al/Ni/Au was evaporated on the epitaxial layer, and then annealed at 850 °C in  $\text{N}_2$  atmosphere for 50 seconds to form the source and drain ohmic contact; ion implantation isolation process was adopted to effectively isolate the active region; using three-layer photoresist technology and electron beam lithography technology to complete the manufacture of T-shaped gate; completing the metal wiring, using PECVD tech-



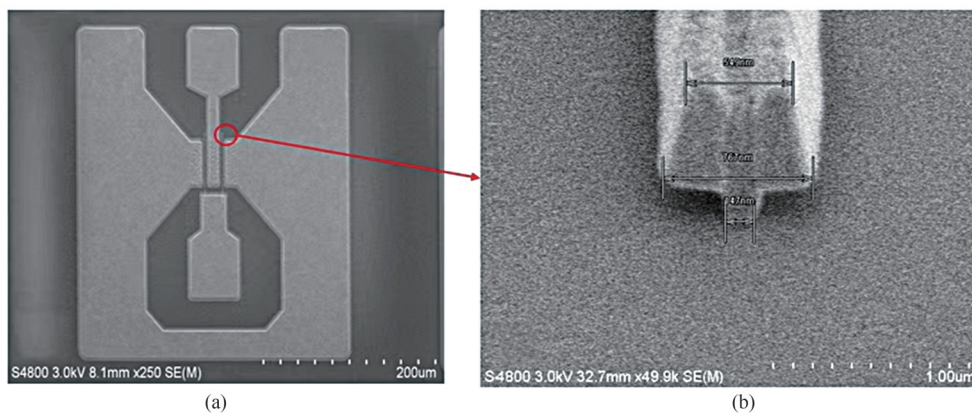
(a)



(b)

Fig. 1 (a) Simulation diagram of  $\text{SiN}_x/\text{AlN}/\text{GaN}$  heterostructure; (b)  $\text{SiN}_x/\text{AlN}/\text{GaN}$  2DEG density and heterostructure energy band simulation diagram

图 1 (a)  $\text{SiN}_x/\text{AlN}/\text{GaN}$  异质结仿真结构; (b)  $\text{SiN}_x/\text{AlN}/\text{GaN}$  2DEG 面密度及能带仿真图



(a)

(b)

Fig. 2 (a) Scanning electron microscopy(SEM) image of the two-finger device; (b) "T" gate structure of SEM  
图 2 (a) 两指器件扫描电镜观测图; (b) SEM "T" 型栅结构

nology to deposit the SiN<sub>x</sub> passivation layer; making the air bridge and the thinning and back hole of the device.

## 2 Results and discussions

### 2.1 Surface state measurement

DLTS is an effective means to detect impurities and defects in the semiconductor at a deep level, which can obtain lots of information such as trap concentration and capture cross section<sup>[4]</sup>.

In order to determine the defect information of gate dielectric interface states in MIS-HEMTs, constant capacitance deep level transient spectroscopy (CC-DLTS) technique was used to detect electron capture and emission processes near gate dielectric. Transient testing of devices in the temperature range of 10-400 K was completed using the Phystech GmbH FT-1030 DLTS system with a capacitance measurement frequency of 1 MHz, combined with the accompanying Lakeshore test stand.

In the CC-DLTS test mode, the SiN<sub>x</sub>/AlN/GaN MIS diode was biased at the pulse height  $U_H = U_P - U_R = 3.5$  V to extract the interface information of the device. The Arrhenius analysis and fitting curve are shown in Fig. 3 (a), and the energy level depth of the defect  $E_C - E_T$  is about  $0.23 \pm 0.01$  eV. The capture cross section is about  $3.05 \times 10^{-19} \text{ cm}^2$ , and the density distribution of extracted interfacial state  $N_{ss}$  is shown in Fig. 3 (b) below. It can be seen from the figure that the extracted interfacial state concentration  $N_{ss}$  decreases from  $3 \times 10^{11} \text{ cm}^{-2} \text{ eV}^{-1}$  at  $T = 10$  K to  $1.5 \times 10^{10} \text{ cm}^{-2} \text{ eV}^{-1}$  at  $T = 400$  K. With the increase of the pulse width  $t_p$ , the signal has a small change range. Combined with the defect energy level information obtained by Arrhenius linear fitting, the measured trap concentration is the interface states at the SiN<sub>x</sub>/AlN interface in MIS structure.

In 2021, Fuqiang Guo<sup>[5]</sup> *et al.* in Microelectronics Institute of Chinese Academy of Sciences used in situ low-damage NH<sub>3</sub>/N<sub>2</sub> remote plasma RPP technology to improve the surface morphology and improve the interface quality of the gate dielectric. They also used PEALD technology to deposition SiN<sub>x</sub> gate dielectrics and developed SiN<sub>x</sub>/AlGaIn/GaN MIS-HEMTs. CC-DLTS measurements showed that the interfacial state concentration  $N_{ss}$  decreased from  $1 \times 10^{13} \text{ cm}^{-2} \text{ eV}^{-1}$  to  $3.4 \times 10^{11} \text{ cm}^{-2} \text{ eV}^{-1}$  after RPP. In contrast, in this paper, the AlN thin barrier without etching process and MOCVD technology was used to grow SiN<sub>x</sub> gate dielectrics in situ, the interface damage and traps were effectively reduced while simplifying the process steps, and the interface concentration  $N_{ss}$  was reduced by 1–2 orders of magnitude.

### 2.2 The DC and small-signal RF measurements

The semiconductor parameter analyzer was used to measure DC, small signal and other basic electrical properties of the device with 50  $\mu\text{m}$  gate width and 4  $\mu\text{m}$  source-drain spacing. The specific results are shown in Fig. 4.

From the current and voltage measurements in Fig. 4(a), it can be seen that the maximum saturation current of  $V_{gs} = 2$  V is 2.2 A/mm, and the on-resistance ( $R_{on}$ ) is  $1.89 \Omega \cdot \text{mm}$ , due to the strong polarization effect of

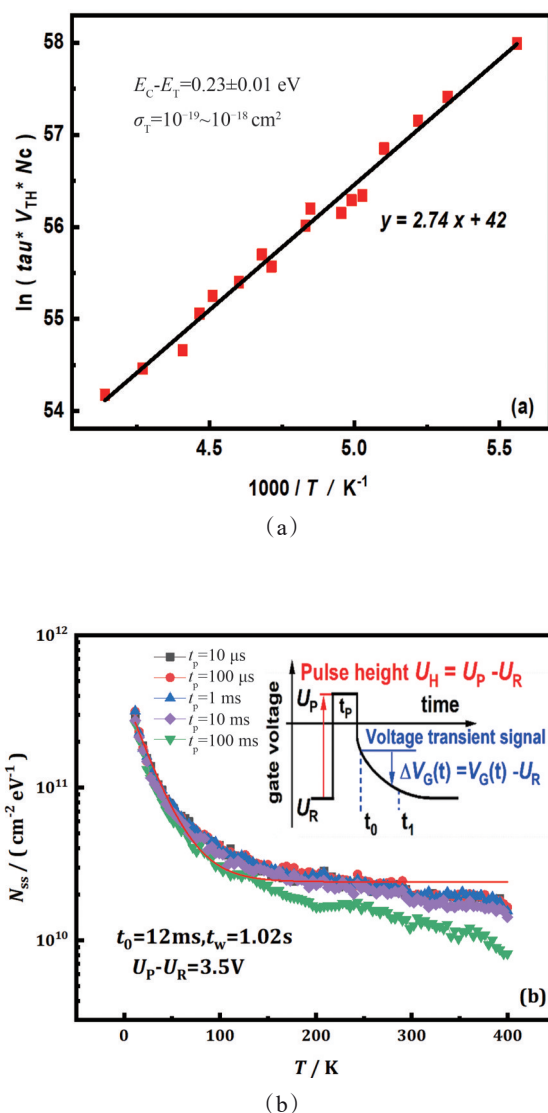


Fig. 3 Measurements of device surface: (a) fitting curve of Arrhenius analysis; (b) density distribution of interfacial  $N_{ss}$ . 图3 器件表面测试: (a) Arrhenius 分析拟合曲线; (b) 界面态  $N_{ss}$  的密度分布

the thin barrier AlN, the device exhibits an excellent current output capacity. As can be seen in Fig. 4(b) of the transfer characteristics of the device, When  $V_{ds}$  is 6 V, the maximum transconductance of the device is 503 mS/mm, and it can be seen from the comparison in the figure that the transconductance of  $V_{ds} = 6$  V has a larger transverse swing, indicating that the device has better linearity and stronger signal transfer ability under this bias condition. Under the condition of  $V_{ds}$  being 6 V, the first-order and second-order derivatives of the transconductance gate-source voltage ( $V_{gs}$ ) are obtained, and the curves of  $G_m$ ,  $G_m'$  and  $G_m''$  are shown in Fig. 4(c), where the bias conditions corresponding to the intersection of the second derivative  $G_m''$  and the coordinate axes show good linearity and noise<sup>[7]</sup>. Subsequently, the measurement point  $V_{gs} = -4.1$  V nearest to the intersec-



tion point was selected for the subsequent noise measurement.

Under the condition of  $V_{ds}$  being 6 V and  $V_{gs}$  being -3 V, the frequency characteristics of the single-finger device were obtained by scanning the  $S$  parameter from the frequency range of 0.1-40 GHz. The measurements showed that the maximum current cutoff frequency ( $f_T$ ) of the device was 65 GHz and the maximum power cutoff frequency ( $f_{MAX}$ ) was 123 GHz under this measurement condition, which ensured the application requirements of the device in the millimeter wave frequency band.

### 2.3 Noise measurements

In order to better evaluate the noise performance of the device, PNA-X vector network analyzer was used based on the cold source method to perform on-chip measurements on the minimum noise figure and gain of the device with a gate width of  $50 \times 2 \mu\text{m}$  and source-drain spacing of  $2.4 \mu\text{m}$ . The DC bias conditions were drain voltage ( $V_{ds}$ ) of 9 V, gate voltage ( $V_{gs}$ ) of -4.1 V, and measurement frequency range was 8-40 GHz. The measurement results are shown in Fig. 5(a) below. The experimental results showed that  $NF_{min}$  of the device satisfied the linear fitting relationship with the measurement frequency.  $NF_{min}$  was 1.07 dB and the gain was 9.93 dB at 40 GHz, which showed superior noise and gain performance. On this basis, the gate voltage of -4.1 V was

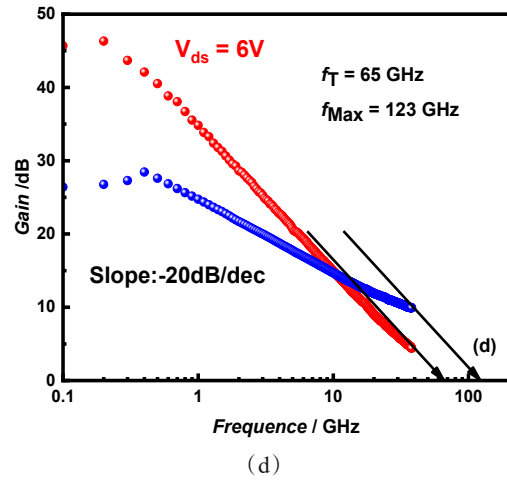
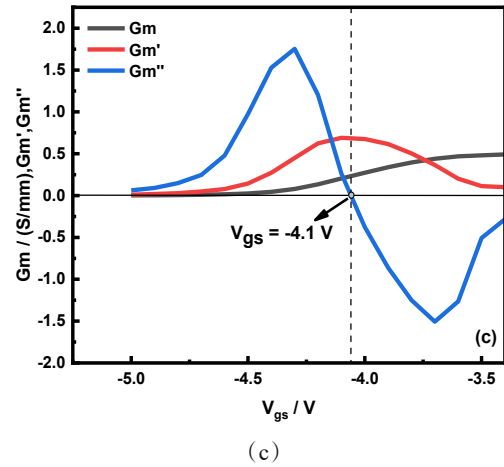
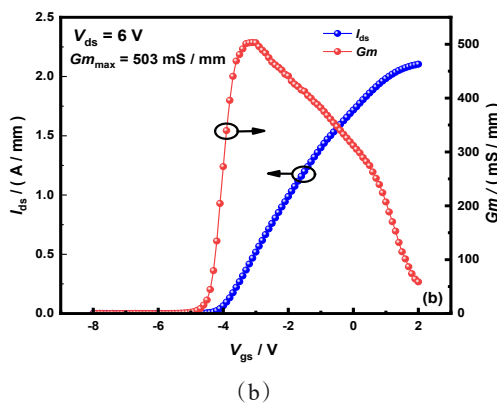
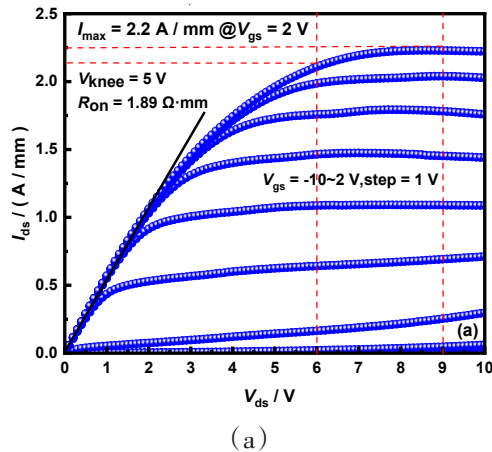


Fig. 4 Basic electrical test of the device: (a) output  $I$ - $V$  curves; (b) transfer and transconductance curves; (c)  $V_{ds} = 6$  V transconductance, first and second derivative curves of transconductance with respect to  $V_{gs}$ ; (d) small signal test curve

图4 器件的基本电学测试:(a)输出电流  $I$ - $V$  曲线;(b)转移和跨导曲线;(c) $V_{ds}=6$  V时,跨导相对于  $V_{gs}$  的一阶和二阶导数曲线;(d)小信号测试曲线

maintained, and the noise and gain of the device at 30 GHz and 40 GHz were measured by changing  $V_{ds}$  (1-10 V). The changes are shown in Fig. 5(b). The gain of the device tended to increase steadily with the rapid increase of  $V_{ds}$ , while  $NF_{min}$  remained at a relatively low level.  $NF_{min}$  of  $V_{ds}$  in the middle range (3-9 V) was stable at 0.85 dB at 30 GHz, and the low noise performance of 1.25 dB was also maintained at 40 GHz.

### 2.4 Linearity measurement

As a crucial component of RF reception front end, the anti-interference capability of the low noise device itself is the key index to evaluate the performance of the device. Therefore, the two-tone linearity of the device was measured in this paper. Based on the load traction system, a PNA-X vector network analyzer was used to provide signals with a frequency interval  $\Delta f$  of 1 MHz and a center frequency of 30 GHz. Devices with the gate

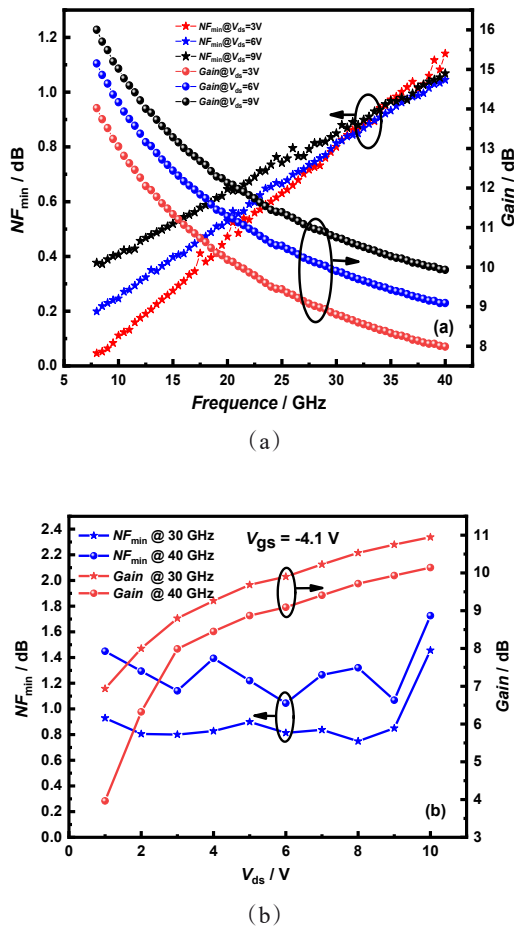


Fig. 5 (a) Noise and gain curves of fixed bias devices; (b) variation curves of noise and gain with source-drain voltage  
图5 (a) 固定偏置下噪声增益曲线; (b) 噪声增益随源漏偏压的变化曲线

width of  $50 \times 2 \mu\text{m}$  and source-drain spacing of  $2.4 \mu\text{m}$  were also selected. In order to compare, the devices were biased at  $V_{ds} = 3 \text{ V}$  and  $6 \text{ V}$ , and static working current was  $40 \text{ mA/mm}$ .

It can be seen from the figure that the input power of the device is in the range of  $-10 \text{ dBm}$  to  $10 \text{ dBm}$ . When  $V_{ds} = 3 \text{ V}$ ,  $OIP3$  was  $28.5 \text{ dBm}$  and  $OIP3/P_{dc}$  was  $7.3 \text{ dB}$ . When the device was biased at  $V_{ds} = 6$ , the maximum  $OIP3$  of the device was  $32.6 \text{ dBm}$ , and  $OIP3/P_{dc}$  had better linearity than  $11 \text{ dB}$  at  $-10 \text{ dBm}$  input power.

In order to better evaluate the performance of SiN<sub>x</sub>/AlN/GaN MIS-HEMTs, such as noise, gain and linearity, parameters selected in this paper are compared with those reported at home and abroad, as shown in Table 2. At present, there are relatively few articles at home and abroad that pay attention to the noise and linearity of low noise devices at the same time. The SiN<sub>x</sub>/AlN/GaN MIS-HEMTs reported in this paper not only have the same linearity level as those at home and abroad, but also have excellent noise performance.

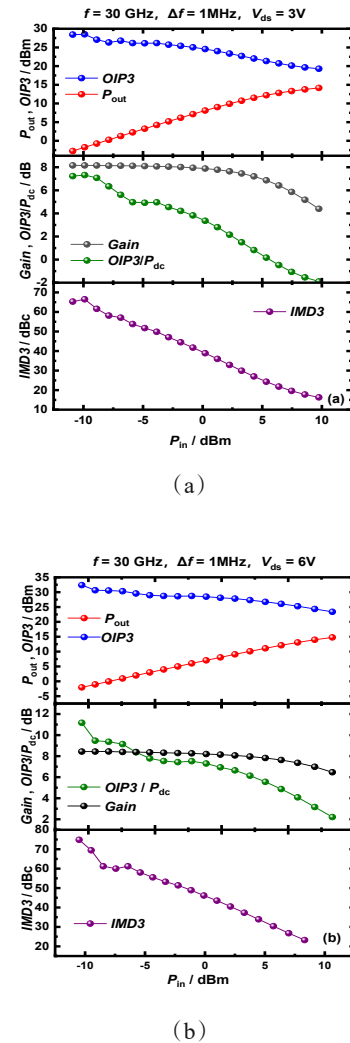


Fig. 6 (a) Measurements of linearity of devices at  $V_{ds} = 3 \text{ V}$ ; (b) measurements of devices at  $V_{ds} = 6 \text{ V}$   
图6 (a)  $V_{ds} = 3 \text{ V}$ 时器件线性度测试结果; (b)  $V_{ds} = 6 \text{ V}$ 时器件线性度测试结果

Table 1 Bias conditions and results for dual tone measurements

表1 双音测试偏置条件和测试结果

$V_{ds} (\text{V})$	Zload	$OIP3 (\text{dBm})$	$OIP3/P_{dc} (\text{dB})$	Gain (dB)
3	$72.7 + 0.8j$	28.5	7.3	8.2
6	$62.5 + 57.6j$	32.4	11.2	8.4

### 3 Conclusions

In this paper, AlN/GaN MIS-HEMTs applied in the millimeter wave band were fabricated. Based on the basic structure and fabrication process of the device, the MIS-HEMTs with high quality interface states were obtained by using MOCVD in situ growth technology to prepare epitaxial SiN<sub>x</sub> gate dielectrics. At the same time, the trap information of SiN<sub>x</sub>/AlN interface of the device was obtained by CC-DLTS measurement. The traps-level

**Table 2 Comparison of performance of low noise devices reported for Millimeter-wave**  
**表 2 已报道的毫米波低噪声器件性能对比**

Paper	Frequency /(GHz)	$NF_{min}$ /(dB)	Gain/(dB)	$OIP3$ / (dBm)	$OIP3$ / $P_{dc}$
2012 <sup>[1]</sup>	36	0.97	7.5	–	–
2019 <sup>[6]</sup>	30	–	–	35	11.4
2020 <sup>[7]</sup>	30	–	12.7	32	15
2020 <sup>[3]</sup>	30	2.2	5.0	>31	>8.2
2022 <sup>[8]</sup>	30	1.9	10	40	20
this paper	30	0.85	10.75	32.60	>11
	40	1.07	9.97	–	–

depth was 0.236 eV and the capture cross-section was  $3.06 \times 10^{-19} \text{ cm}^{-2}$ , the extracted interface state density was  $10^{10}$  to  $10^{12} \text{ cm}^{-2} \text{ eV}^{-1}$ . The device with a gate length of 0.15  $\mu\text{m}$  had  $I_{dmax}$  of 2.2 A/mm at  $V_{gs}$  of 2 V, the peak  $Gm$  was 506 mS/mm.  $f_t$  and  $f_{Max}$  of the device at  $V_{ds}$  of 6 V were 65 and 123 GHz, respectively. The results of DC and small signal showed that the device had good output, transfer characteristics and application potential in the millimeter wave band. Benefited from the strong polarization effect of AlN/GaN and the high-quality interface state of SiN<sub>x</sub>/AlN, the devices have excellent noise performance and linearity.  $NF_{min}$  of the device was 1.07 dB and the gain was 9.93 dB at 40 GHz. When  $V_{ds}$  was 6 V, the third-order intermodulation output power ( $OIP3$ ) of the device was 32.6 dBm, and  $OIP3/P_{dc}$  reached 11.2 dB. Compared with the noise and linearity of low noise devices reported at present, some performance improve-

ments have been made in this paper. In conclusion, the MIS-HEMTs fabricated in this paper based on SiN<sub>x</sub>/AlN/GaN heterostructure have excellent performances such as low noise and high linearity, and are high-performance devices working in the RF front end.

References

[1] Medjdoub F, Tagro Y, Zegaoui M, *et al.* Sub-1-dB Minimum-Noise-Figure Performance of GaN-on-Si Transistors Up to 40 GHz [J]. *Electron Device Letters*, IEEE, 2012, **33**(9):p.1258–1260.

[2] Lu X, Ma J, Jiang H, *et al.* Low trap states in in situ SiN<sub>x</sub>/AlN/GaN metal-insulator-semiconductor structures grown by metal-organic chemical vapor deposition [J]. *Applied Physics Letters*, 2014, **105**(10):287–305.

[3] Choi Woojin, Chen Renjie, Levy Cooper, *et al.* Intrinsically Linear Transistor for Millimeter-Wave Low Noise Amplifiers [J]. *Nano letters*, 2020, **20**(4):2812–2820.

[4] Yao Y, Jiang Q, Huang S, *et al.* Identification of bulk and interface state-induced threshold voltage instability in metal/SiN<sub>x</sub> (insulator)/AlGaIn/GaN high-electron-mobility transistors using deep-level transient spectroscopy [J]. *Japanese Journal of Applied Physics*, 2021, **119**:233502.

[5] Guo F, Huang S, Wang X, *et al.* Suppression of interface states between nitride-based gate dielectrics and ultrathin-barrier AlGaIn/GaN heterostructure with in situ remote plasma pretreatments [J]. *Applied Physics Letters*, 2021, **118**(9):093503.

[6] M. Guidry, B. Romanczyk, H. Li, *et al.* "Demonstration of 30 GHz  $OIP3/PDC > 10$  dB by mm-wave N-polar Deep Recess MISHEMTs," 2019 14th European Microwave Integrated Circuits Conference (EuMIC), Paris, France, 2019, pp.64–6.

[7] Shrestha P, Buckwalter J F, Mishra U K, *et al.* High Linearity and High Gain Performance of N-Polar GaN MIS-HEMT at 30 GHz [J]. *IEEE Electron Device Letters*, 2020, PP(99):1–1.

[8] M. Guidry, P. Shrestha, Wenjian Liu, *et al.* Improved N-polar GaN mm-wave Linearity, Efficiency, and Noise [C]. 2022 IEEE/MTT-S International Microwave Symposium-IMS 2022, Denver, CO, USA, 2022, pp. 291–294.